THE JOURNAL OF PHYSICAL CHEMISTRY B

 VOLUME 108, NUMBER 2, JANUARY 15, 2004

# LETTERS

## Uniform-Diameter Single-Walled Carbon Nanotubes Catalytically Grown in Cobalt-Incorporated MCM-41

**Dragos Ciuparu,* Yuan Chen, Sangyun Lim, Gary L. Haller, and Lisa Pfefferle**

*Department of Chemical Engineering, Yale University, New Haven, Connecticut 06520*

*Received: August 18, 2003; In Final Form: November 4, 2003*

Single-walled carbon nanotubes of uniform diameter were grown in cobalt-substituted MCM-41 molecular sieves templated with C12 and C16 alkyl chains to result in pore diameters of 2.6 and 3.3 nm, respectively. The narrow diameter distribution of the tubes grown was probed by Raman, UV−visible, and NIR spectroscopy, as well as by high-resolution transmission electron microscopy. Tube diameters have been observed to vary with the size of the Co clusters formed during carbon deposition, as measured by extended X-ray absorption fine structure (EXAFS). It is proposed that the diameter of the carbon nanotubes grown in MCM-41 catalysts is controlled by the size of the metallic clusters formed in the template. Because MCM-41 catalysts of different pore diameter form Co clusters of different sizes, this mechanism can be exploited to grow carbon nanotubes of uniform, preselected diameters.

As widely reported,[1−5] carbon nanotubes exhibit technologically important electronic properties potentiating new device development. They can be found in both metallic and semiconducting structures. The structure of the single-walled nanotube (SWNT) is defined by how the graphitic sheet is aligned in the rolled up configuration. Metallic (m) nanotubes can carry extremely large current densities;[6] semiconducting (s) nanotubes can be electrically switched on and off as field-effect transistors (FETs) (e.g., ref 6). Most electronic applications of carbon nanotubes require aligned SWNTs that are reasonably homogeneous in diameter, length, and electronic properties. Odom et al.[7] used scanning tunneling microscopy (STM) to correlate atomic structure with electronic properties of SWNTs. They found that the electronic properties correlate both with the diameter and helicity (twist). This important work illustrates why control of SWNT diameter and structure is of crucial importance for the development of new electronic devices based on SWNTs.

The current state of the art of SWNT synthesis is given in a recent review.[8] Processes now exist that yield 90% selectivity for SWNT in scalable processes (for example, Dai and co-workers,[9,10] Resasco and co-workers,[11] Smalley and co-workers[12]). Cleaning, separation, and alignment steps are required for use in electronic applications. Due to the harsh reaction conditions required for SWNT synthesis, traditionally prepared metallic particulate catalysts will not likely lead directly to the desired very narrow diameter distributions. Catalysts, particularly metal catalysts, restructure and sinter leading to the formation of multifaceted crystals, each facet potentially initiating the growth of a SWNT and thus a spread of particle sizes and multiple nanotubes from each particle leading to heterogeneity in diameter and structure (e.g., see refs 13 and 14).

An important recent development is the use of zeolite channels as templates to synthesize SWNTs.[15−18] An intriguing finding from this zeolite work is that interactions with the channel walls during nanotube formation were observed to lead to selection of a particular nanotube structure.[17] If control could be achieved for a range of diameters, this could provide an important tool for controlling SWNT properties. Zeolites,

* Corresponding author. Phone: 203-432-4383. Fax: 203-432-4387. E-mail: dragos.ciuparu@yale.edu.

10.1021/jp036453i CCC: $27.50 
Published on Web 12/16/2003

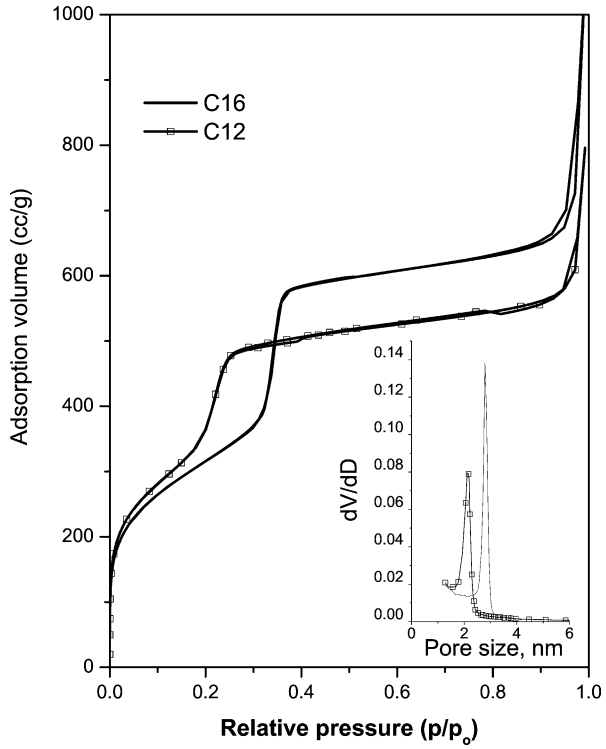


**Figure 1.** Physisorption isotherms measured with fresh C12 and C16 templates. The inset shows the pore size distribution derived from the desorption isotherms by the modified BJH method.[31]

however, because of their lack of composition and pore size flexibility, are not an ideal choice for a SWNT template. As used here, template does not imply a one to one pattern transfer of the template structure to the SWNT. Templating of the SWNTs is exercised through the influence of the pore wall on the size of the nucleating metal cluster. The ideal template material should allow independent control of both composition and channel size. The M41S class of mesoporous materials developed by Mobil[19] is ideal in that the walls are amorphous and structured pore arrangements with pore sizes from 1.5 to 4 nm can be produced independent of metal substitution in the framework (for dilute substitutions). We have found the wall thickness to be relatively uniform in this pore size regime at approximately 1 nm.

In this contribution, we demonstrate the formation of uniform-size SWNTs controllable by the properties of a cobalt-substituted template having a parallel system of pores. The nanotubes are uniform in diameter and spacing. The catalytically active site or site precursor is produced by MCM-41 framework substitution with cobalt. The catalytic component is highly dispersed in the pore wall and its oxidation state can be controllably modified by varying pretreatment conditions. The mesoporous molecular sieve used as a catalytic template for SWNT growth was produced using a surfactant-templated synthesis modified from the original Mobil method to improve structural order. The synthesis and characterization of the Co−MCM-41 is discussed elsewhere.[20] Two different Co−MCM-41 catalysts were used in this study, one with pore size by high-resolution transmission electron microscopy (HR-TEM) of 3.3 nm and the other with a pore size of 2.6 nm. The pore size distribution in the Co−MCM-41 catalysts measured by nitrogen physisorption in a static volumetric instrument Autosorb-1C (Quanta Chrome) is on the order of 0.1 nm full width at half-maximum, as observed in Figure 1. It should be mentioned that similar measurements performed with the MCM-41 templates after reduction with hydrogen at 500 °C and after carbon deposition

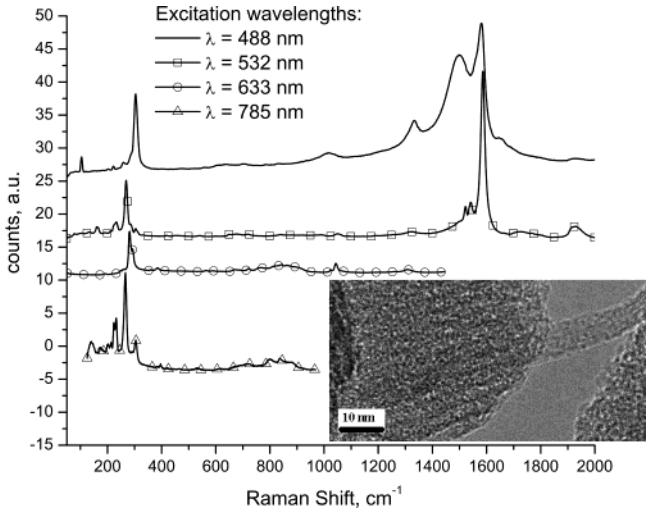


**Figure 2.** Raman spectra recorded at different excitation wavelengths for unpurified SWNT samples grown without hydrogen prereduction in the C16 catalytic template. TEM inset shows SWNTs uniform in size evolving from the pores of the Co−MCM-41 catalyst with hydrogen prereduction.

and subsequent removal by oxidation showed minor modifications of structure and pore size distribution, suggesting that these templates have good structural stability under both reduction and oxidation conditions.[20]

Single-walled carbon nanotubes were synthesized by CO disproportionation. The Co−MCM-41 catalyst was packed in a 10 mm internal diameter quartz reactor, heated in flowing oxygen to 750 °C, purged for 10 min with argon, and then reacted with CO for 2 h. In an optimized reaction strategy, before reaction the catalyst was heated in flowing hydrogen to 773 K at 20 K/min and held at that temperature for 15 min. Subsequently, the reactor was flushed with Ar, and the temperature was further raised at 20 K/min to 1023 K under flowing Ar. The Boudouard reaction was carried out for 1 h at 1023 K in a pure CO atmosphere; then the catalyst was again flushed with Ar and cooled to room temperature in Ar.

As-synthesized samples and purified carbon nanotube samples were characterized by HR-TEM and Raman, UV−vis, and near-IR spectroscopy. The purification process consisted of template removal by ultrasonication for 4 h in 48% HF to dissolve the silica and the cobalt from the sample. Nitrogen physisorption was also used to determine the diameter of the tubes removed from the catalyst and to measure the pore size distribution of the templates at different stages in the process.

The resonant Raman spectra in Figure 2 recorded at four different excitation wavelengths (488, 532, 633, and 785 nm) with a C16 catalyst without hydrogen prereduction indicate that the samples have a uniform diameter. The main peaks correspond to tube diameters ranging from 7.7 to 8.9 nm. It should be mentioned that spectra (not shown) recorded at the 532 nm excitation wavelength with a sample prepared by the optimized reaction strategy with hydrogen prereduction show a single peak at approximately 250 cm$^{-1}$. This indicates the nanotubes are of uniform size. This conclusion is also supported by analysis of over 60 locations on several TEM grids. An illustrative image of a tube bundle grown with a hydrogen-prereduced C16 catalyst is given in the inset of Figure 2. The inner diameter of SWNTs obtained using the optimized reaction strategy with the C16 template varied between 0.84 and 0.86 nm, while those grown on the C12 template averaged 0.67 nm in diameter. The Raman spectra shown in Figure 2 were recorded with an unpurified, as-synthesized sample without previous cleaning or any other

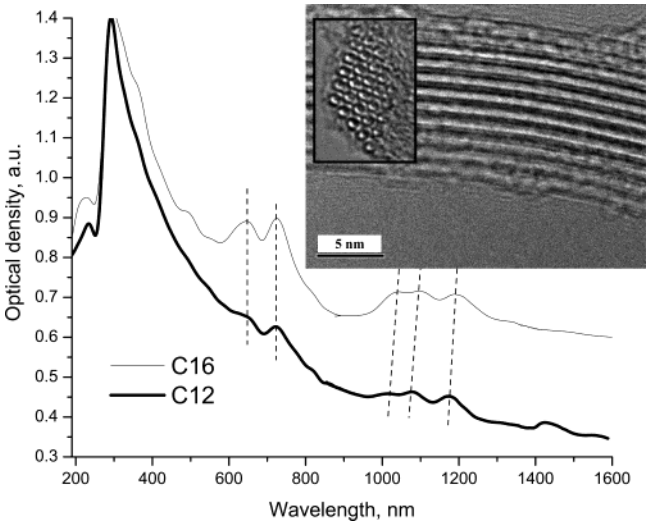


**Figure 3.** UV-visible and NIR spectra recorded for unpurified SWNT samples grown in C12 and C16 templates with hydrogen prereduction. TEM inset shows the uniformity of the SWNTs grown in the C12 template.

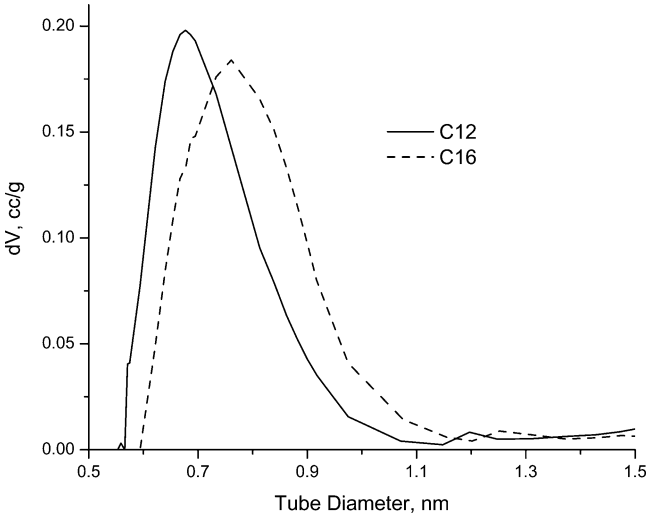


**Figure 4.** Tube size distribution measured for HF-purified SWNT samples by nitrogen physisorption.

form of postsynthesis treatment. These spectra also confirm high selectivity to SWNT with very little amorphous carbon: the area of the spectra indicating disordered carbon at 1350 $cm^{-1}$ is reasonably flat. The ratio between the D band, characteristic for the disordered (amorphous) carbon, and the G band, attributed to ordered carbon, to our knowledge is much higher than those previously reported for unpurified SWNT samples.[21]

Figure 3 shows the UV−vis and near-IR spectra for the nanotubes grown in hydrogen-prereduced C12 and C16 catalysts, along with a TEM image showing the diameter uniformity of the SWNTs grown in the hydrogen-prereduced C12 template. The peak complex in the visible region was previously assigned to the second Van Hove transition of semiconducting tubes, while the peaks in the NIR region were attributed to the $E_{11}$ interband transitions of the semiconducting tubes.[22] The blue shift of the $E_{11}$ transition of the C12 sample in the NIR region is direct evidence for a smaller diameter of SWNTs grown in the C12 template.[22,23] However, the spectral feature in the visible domain is not shifted as much. Assignments are not necessarily definitive because adsorbates induce significant changes in the spectral features of the smaller nanotubes.

The diameter distribution measured by nitrogen physisorption on purified SWNT samples removed from the template by HF treatment is given in Figure 4. The average diameter values measured in the physisorption experiment are 0.68 and 0.76 nm for C12 and C16, respectively, thus showing smaller SWNT diameter for the template with smaller pore diameter. The differences between the physisorption measurements and the TEM results are most likely due to the assumption that the wetting angle (used in the Kelvin equation) for liquid nitrogen on carbon is zero. Most liquids with low surface tension have a smaller contact angle on graphite than on silica. Therefore, the nanotube diameter may be underestimated because it was calculated using the same angle as that used for the template material, which is mostly silica.[20] In addition, liquid nitrogen has different contact angles on walls of different pore diameters because of the pore curvature. Smaller pores contact a larger area with the nitrogen molecule than wider pores, resulting in smaller contact angle and underestimation of nanotube diameter. These nanoscale phenomena are likely responsible for the differences observed between the diameter measurements by TEM and nitrogen physisorption. Also, the relatively wider distribution of tube diameters observed in the physisorption results is most likely due to defects created in the SWNT structure during the HF treatment and to the interstitial spaces between tubes. The presence of defects may also create interstitial spaces that act as micropores during physisorption measurements.

On the basis of investigation of silica-supported Co−Mo catalysts, Resasco and co-workers[11] proposed that the high selectivity observed for Co−Mo catalysts as compared to monometallic Co catalysts is due to the stabilization effect of molybdenum, which impedes rapid Co reduction, thus leading to a slow Co reduction and formation of small Co clusters highly selective for SWNT synthesis. We propose that a similar role may be played by the silica matrix in our Co-substituted MCM-41 catalytic template.

The diameters of the SWNT produced are significantly smaller than the template pore diameter; however, the SWNT diameter correlates with the pore diameter; therefore, it is likely that control is obtained through the effect of the pore size on the size of the metal clusters formed during reduction. This is also consistent with the observation that harsher conditions are required to reduce cobalt in the MCM-41 framework and the reducibility decreases with the pore diameter. To test this hypothesis, catalyst samples previously exposed to the SWNT growth as discussed above were investigated by X-ray absorption fine structure (XAFS).

X-ray adsorption data of fresh Co−MCM-41, Co metal foil, and C12 and C16 Co−MCM-41 loaded with carbon were measured at beam line X 18-B equipped with a Si(111) crystal monochromator at the National Synchrotron Light Source at Brookhaven National Laboratory. The intensity of the incident beams ($I_0$) was measured with a 30 cm long ion chamber filled with pure $N_2$. X-ray adsorption data were collected in transmission mode by scanning from 200 eV to 16 keV above the Co K edge. The $I_T$ value was measured with the ion chamber filled with a 4:1 $N_2$ in Ar mixture. Samples of approximately 45 mg of Co−MCM-41 were pressed into a rectangular wafer (ca. 1.5 cm × 1 cm) to form 0.5 mm thick pellets. The wafer was then placed between the ion chambers. The spectra were obtained by averaging three scans for each sample.

The X-ray absorption data were analyzed using the procedure described elsewhere.[24] First, the smooth isolated-atom background function was removed from the experimental X-ray absorption coefficient data by FEFFIT.[25] Then theoretical

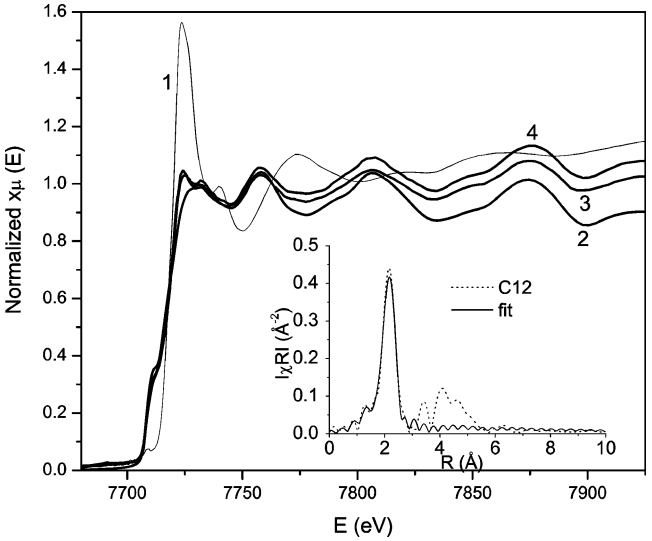


**Figure 5.** Near-edge spectra of Co K edge ($E_0$ = 7709 eV): (1) spectrum for the fresh Co−MCM-41; (2) spectrum for metallic cobalt foil; (3, 4) C12 and C16, respectively, Co−MCM-41 samples after SWNT growth. The inset shows an example of fitting the spectra with the model.

photoelectron scattering amplitudes and phase shifts of Co metal were calculated for a model structure. Finally, the theoretical extended X-ray absorption fine structure (EXAFS) signal of Co metal was fit to the experimental EXFAS data of C12 and C16 Co−MCM-41 (after reaction) in *R*-space by Fourier transforming both the theoretical and the experimental data using FEFF6 from the University of Washington.[26]

The near-edge spectra (XANES) of Co K edge ($E_0$ = 7709 eV) shown in Figure 5 suggests Co in the fresh Co−MCM-41 sample is in the oxidized state. However, after reaction, the XANES spectrum beyond the white line is almost identical to that of a Co foil; thus, the cobalt was mostly reduced after carbon deposition. Fitting the spectra recorded with C12 and C16 with the Co metal theoretical model, we obtained curves similar with the one depicted in the inset of Figure 5 for C12. The coordination numbers determined for C12 and C16 were 6.1 and 6.8, respectively. The differences in bond distances with respect to the theoretical references ($\Delta T$) were 0.015 and 0.016, respectively, indicating that the fit is within acceptable limits.

The coordination number of particles smaller than 5 nm is a strong and nonlinear function of the particle diameter. This property has been widely used in EXAFS analysis to determine the size of nanoparticles.[27,28] As discussed by Frenkel,[24] although the geometry of clusters with different sizes, shapes, or lattice symmetries will generate different coordination numbers, the (111)-truncated hemispherical cubic octahedron model provides the best approximation for the relation between the average coordination number and the size of nanoparticles. We have built close packing models for cobalt (hcp) to determine the correlation depicted in Figure 6 between the average coordination number of the cobalt clusters and their diameters.

The coordination number determined from the EXAFS spectra of hexagonally closed packed Co atoms in the metallic clusters present in the C12 and C16 samples after SWNT growth for 1 h in pure CO at 750 °C are plotted on the theoretical curve showing the dependence of the cluster size on the coordination number of cobalt atoms in each cluster. These results suggest that our catalyst contains clusters with no more than 20 or 30 Co atoms, respectively, for the C12 and C16 samples. Since the EXAFS spectra shows a volume-average coordination number, the actual metallic cluster in the MCM-41 pore may

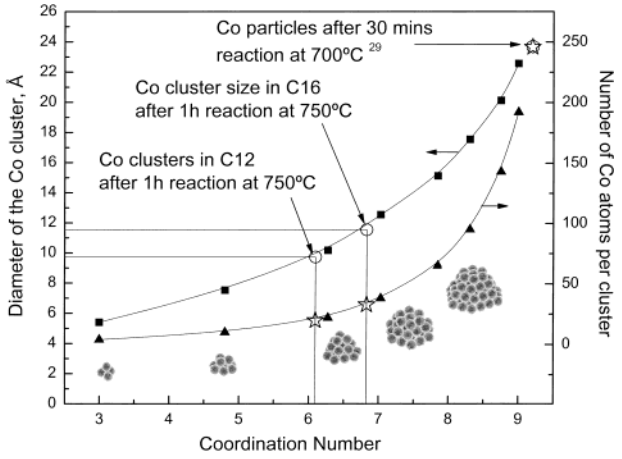


**Figure 6.** The upper limit of the diameter of the Co clusters determined from the analysis of the EXAFS spectra recorded for C12 and C16 samples exposed to pure CO at 750 °C for 1 h. Cobalt cluster sizes observed by Resasco[29] for a silica-supported Co−Mo catalyst exposed to CO at 700 °C for 30 min are given for comparison.

be even smaller than these because metallic particles formed outside the pore system are more mobile and can grow to larger sizes than those inside the pores. These results are consistent with TEM investigations that did not reveal the presence of metallic particles in samples after carbon deposition. It is therefore likely that the SWNT diameter is controlled by the size of the MCM-41-stabilized Co cluster, which fits in the range of the tube sizes determined from TEM images. If this is the case, we should note that the cobalt clusters produced with the MCM-41 catalyst are significantly smaller than the 9.2 coordination number observed by Resasco et al. with Co−Mo/$SiO_2$ catalysts, although our catalyst was exposed 30 min longer to even harsher reaction conditions (i.e., 750 vs 700 °C in the cited work).[29] Therefore, this catalytic system shows promise of improving selectivity and diameter control of SWNT for large scale applications.

The results presented here suggest that mesoporous molecular sieve templates with metals incorporated in the framework exhibit good structural stability and can be used for growth of ordered SWNT of uniform size and structure at yields and selectivity promising for large scale applications. The Co−MCM-41 catalysts become more reactive after being partially reduced in hydrogen. Reducibility of the catalytic component is strongly affected by the pore diameter of the MCM-41 material. Uniformity of SWNT diameter results most likely from the uniformity of the metallic Co clusters formed in the template. From related work, the size of these clusters appears to be controlled by the radius of curvature of the MCM-41 mesoporous molecular sieve.[30] In conclusion, this contribution shows the potential of mesoporous materials such as MCM-41 to control the properties of SWNT during synthesis.

**Acknowledgment.** We thank DARPA-DSO for the financial support of this project. Partial support of DoE, Office of Basic Energy Sciences, for synthesis of the MCM-41 is also acknowledged. The authors thank Jasco, Inc. for providing multiple excitation wavelengths Raman analysis for our samples.

## References and Notes

(1) Bachtold, A.; Hadley, P.; Nakanishi, T.; Dekker, C. *Science* **2001**, *294*, 1317.

(2) Bockrath, M.; Liang, W.; Bozovic, D.; Hafner, J. H.; Lieber, C. M.; Tinkham, M.; Park, H. *Science* **2001**, *291*, 283.

(3) Collins, P. G.; Zettl, A.; Bando, H.; Thess, A.; Smalley, R. E. *Science* **1997**, *278*, 100.
(4) Ouyang, M.; Huang, J.-L.; Cheung, C. L.; Lieber, C. M. *Science* **2001**, *291*, 97.
(5) Tans, S. J.; Dekker, C. *Nature (London)* **2000**, *404*, 834.
(6) Collins, P. G.; Arnold, M. S.; Avouris, P. *Science* **2001**, *292*, 706.
(7) Odom, T. W.; Huang, J.-L.; Kim, P.; Lieber, C. M. *Nature (London)* **1998**, *391*, 62.
(8) Dai, H. *Acc. Chem. Res.*, in press, available on the web athttp://pubs.acs.org, Articles ASAP.
(9) Cassell, A. M.; Franklin, N. R.; Tombler, T. W.; Chan, E. M.; Han, J.; Dai, H. *J. Am. Chem. Soc.* **1999**, *121*, 7975.
(10) Cassell, A. M.; Raymakers, J. A.; Kong, J.; Dai, H. *J. Phys. Chem. B* **1999**, *103*, 6484.
(11) Resasco, D. E.; Alvarez, W. E.; Pompeo, F.; Balzano, L.; Herrera, J. E.; Kitiyanan, B.; Borgna, A. *J. Nanopart. Res.* **2002**, *4*, 131.
(12) Nikolaev, P.; Bronikowski, M. J.; Bradley, R. K.; Rohmund, F.; Colbert, D. T.; Smith, K. A.; Smalley, R. E. *Chem. Phys. Lett.* **1999**, *313*, 91.
(13) Laplaze, D.; Alvarez, L.; Guillard, T.; Badie, J. M.; Flamant, G. *Carbon* **2002**, *40*, 1621.
(14) Saito, Y.; Okuda, M.; Tomita, M.; Hayashi, T. *Chem. Phys. Lett.* **1995**, *236*, 419.
(15) Tang, Z. K.; Sun, H. D.; Wang, J.; Chen, J.; Li, G. *Bull. Mater. Sci.* **1999**, *22*, 329.
(16) Mukhopadhyay, K.; Koshio, A.; Tanaka, N.; Shinohara, H. *Jpn. J. Appl. Phys., Part 2* **1998**, *37*, L1257.
(17) Sun, H. D.; Tang, Z. K.; Chen, J.; Li, G. *Appl. Phys. A: Mater. Sci. Process.* **1999**, *69*, 381.
(18) Hayashi, T.; Kim, Y. A.; Matoba, T.; Esaka, M.; Nishimura, K.; Tsukada, T.; Endo, M.; Dresselhaus, M. S. *Nano Lett.* **2003**, *3*, 887.
(19) Beck, J. S.; Vartuli, J. C.; Roth, W. J.; Leonowicz, M. E.; Kresge, C. T.; Schmitt, K. D.; Chu, C. T. W.; Olson, D. H.; Sheppard, E. W.; McCullen, S. B.; Higgins, J. B.; Schlenker, J. L. *J. Am. Chem. Soc.* **1992**, *114*, 10834.
(20) Lim, S.; Ciuparu, D.; Pak, C.; Dobek, F.; Chen, Y.; Harding, D.; Pfefferle, L.; Haller, G. *J. Phys. Chem. B* **2003**, *107*, 11048.
(21) Herrera, J. E.; Resasco, D. E. *Chem. Phys. Lett.* **2003**, *376*, 302.
(22) Liu, X.; Pichler, T.; Knupfer, M.; Golden, M. S.; Fink, J.; Kataura, H.; Achiba, Y. *Phys. Rev. B* **2002**, *66*, 045411/1−045411/8.
(23) Chiang, I. W.; Brinson, B. E.; Smalley, R. E.; Margrave, J. L.; Hauge, R. H. *J. Phys. Chem. B* **2001**, *105*, 1157.
(24) Frenkel, A. I.; Hills, C. W.; Nuzzo, R. G. *J. Phys. Chem. B* **2001**, *105*, 12689.
(25) http://cars9.uchicago.edu/ifeffit/ (accessed August 2003).
(26) http://leonardo.phys.washington.edu/feff/ (accessed August 2003).
(27) Via, G. H.; Sinfelt, J. H.; Lytle, F. W. *J. Chem. Phys.* **1979**, *71*, 690.
(28) Greegor, R. B.; Lytle, F. W. *J. Catal.* **1980**, *63*, 476.
(29) Alvarez, W. E.; Kitiyanan, B.; Borgna, A.; Resasco, D. E. *Carbon* **2001**, *39*, 547.
(30) Lim, S.; Ciuparu, D.; Chen, Y.; Pfefferle, L.; Haller, G., manuscript in preparation, 2003.
(31) Barrett, E. P.; Joyner, L. G.; Halenda, P. P. *J. Am. Chem. Soc.* **1951**, *73*, 373.